ELSEVIER

Chemical Geology 233 (2006) 196–216

CHEMICAL GEOLOGY
INCLUDING
ISOTOPE GEOSCIENCE

www.elsevier.com/locate/chemgeo

Chemical systematics of conodont apatite determined by laser ablation ICPMS

Julie A. Trotter [a,b,*], Stephen M. Eggins [a]

[a] *Research School of Earth Sciences, Australian National University, Canberra, ACT, 0200, Australia*
[b] *CSIRO Petroleum, North Ryde, NSW, 2113, Australia*

Received 30 September 2005; received in revised form 25 February 2006; accepted 2 March 2006

Abstract

Minor and trace element compositions of a suite of Ordovician, Silurian, and Permian conodonts have been characterised by laser ablation inductively coupled plasma mass spectrometry (LA-ICPMS). Continuous, high-resolution chemical depth profiles through individual conodont elements reveal systematic compositional differences between the component histologies (albid, hyaline, and basal body tissues). Comparative analyses of contemporaneous bio-apatites (ichthyoliths and inarticulate brachiopods), as well as Holocene and modern fish material, show linear relationships between their respective rare earth element, yttrium, lead, thorium, and uranium compositions, which has implications for their relative permeability and susceptibility to diagenesis. Assessment of LA-ICPMS profiles in the context of histology, general morphological structure, and post-depositional chemical exchange, suggests that conodont albid crown is the least permeable histology, whereas hyaline crown, basal tissue, ichthyoliths, and inarticulate brachiopods are strongly overprinted by the selective uptake of Y–REE–Th–U during diagenesis. Conodont albid crown is therefore more resistant than other bio-apatite histologies to postmortem uptake of Y–REE–Th–U, and trends below detection limits that more closely approach primary conodont compositions. This relationship between sample histology and geochemistry, especially in the context of diagenetic overprinting, demands careful consideration when reconstructing palaeoseawater compositions.

Keywords: LA-ICPMS; Laser ablation; Conodont; Apatite; Geochemistry; Palaeoseawater

1. Introduction

Fossil marine bio-apatites (conodonts and ichthyoliths) have the potential to record palaeoseawater compositions, which can be used to better understand and reconstruct palaeoenvironmental change through geological time. Conodonts are particularly attractive as potential proxies due to their ubiquity, biostratigraphic importance, and temporal range. However, their small size has been a limiting factor for geochemical analysis but recent advances in microanalytical techniques now provide the opportunity to analyse specific histologies within single conodont elements, with both high sensitivity and high spatial resolution. This study has taken this approach to determine the chemical systematics of conodont tissues and thus infer their inherent integrity and susceptibility to diagenesis.

Following initial investigations of conodont apatite chemistry (Pietzner et al., 1968; Wright et al., 1987a,b, 1990), various studies have focused on trace elements

* Corresponding author. Research School of Earth Sciences, Australian National University, Canberra, ACT, 0200, Australia. Tel.: +61261259968; fax: +61261257739.
E-mail address: Julie.Trotter@csiro.au (J.A. Trotter).

0009-2541/$ - see front matter © 2006 Elsevier B.V. All rights reserved.
doi:10.1016/j.chemgeo.2006.03.004

and rare earth element distributions in particular (Wright et al., 1984, 1987b; Bertram et al., 1992; Grandjean - Lécuyer et al., 1993; Girard and Albarède, 1996; Bruhn et al., 1997; Girard and Lécuyer, 2002), strontium isotope compositions (Keto and Jacobsen, 1987; Bertram et al., 1992; Kürschner et al., 1992; Martin and Macdougall, 1995; Diener et al., 1996; Holmden et al., 1996; Ruppel et al., 1996; Ebneth et al., 1997; Trotter et al., 1999; Armstrong et al., 2001; Ebneth et al., 2001), neodymium isotope compositions (Wright et al., 1984; Keto and Jacobsen, 1987; Bertram et al., 1992; Martin and Macdougall, 1995; Holmden et al., 1996, 1998; Felitsyn et al., 1998; Wright et al., 2002) and oxygen isotope compositions (Luz et al., 1984; Geitgey and Carr, 1987; Wenzel et al., 2000; Joachimski and Buggisch, 2002; Joachimski et al., 2004).

Conodonts are carbonate fluorapatite (Pietzner et al., 1968) microfossils and as such are considered to have greater integrity than coeval carbonates. Their ubiquity and rapid evolution throughout Cambrian to Triassic marine sequences underscores their biostratigraphic significance but also makes them attractive as potential geochemical proxies. Conodont 'elements' are believed to be the mineralised remains of the cephalic feeding apparatus of small, extinct, marine animals of controversial affinity. They are morphologically diverse and most commonly represented by crown components comprised of hyaline (translucent) and albid (opaque white) tissues (Fig. 1). Albid crown is variably distributed within cusps and denticles, and typically described as fine-grained with a cancellate unconnected porosity. Hyaline tissue is believed to comprise much larger crystals (<1 μm to >30 μm), has a lamellar structure, and often accommodates secondary precipitates indicating some degree of permeability (Fig. 2). Less frequently preserved are the basal bodies (Fig. 1), the most finely crystalline conodont tissue that may be variably mineralised.

The small size (~0.1 to 3 mm in length) of conodont elements has limited most previous geochemical studies to bulk analyses, and details regarding taxonomy, morphology, and histology of analysed specimens are often lacking. Furthermore, the relative integrities of the component tissues have not been adequately investigated, despite likely differences in their susceptibility to diagenesis. The chemical systematics of conodont apatite and of biogenic apatite in general, including the effects of diagenesis, is not well understood, which reflects the general lack of rigorous and systematic studies. Moreover, research into the

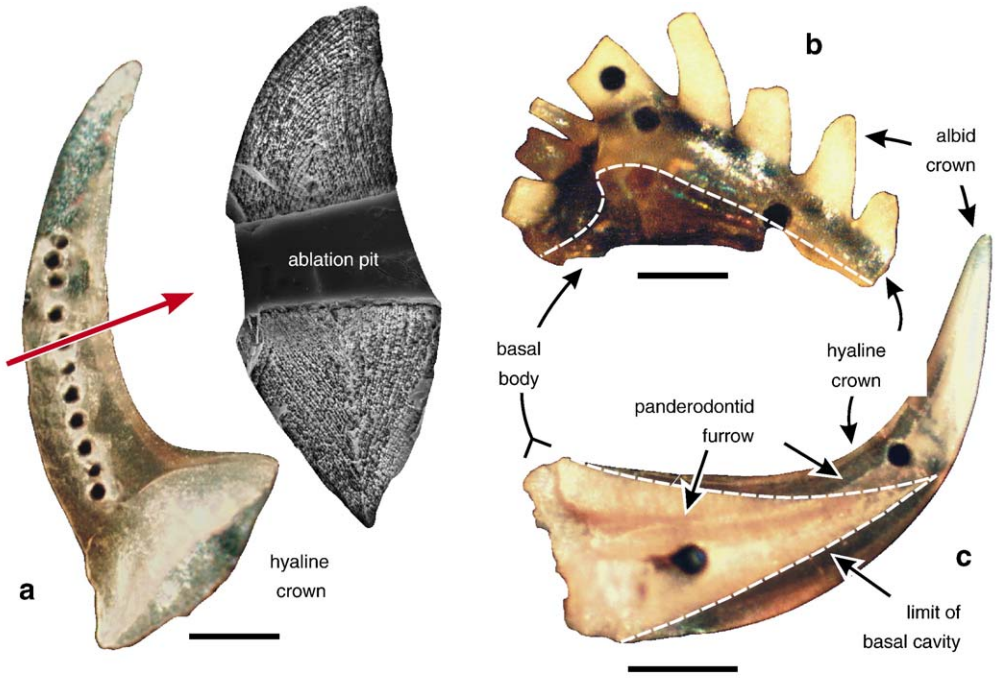

Fig. 1. Conodont mineralised tissues represent by (a) *Drepanoistodus suberectus* (Branson and Mehl): concentric lamellar structure of hyaline tissue dissected by a laser ablation pit (SEM); (b) *Oulodus* sp.: albid crown comprising denticles and cusp, hyaline crown, and densely mineralised basal body indicated by dashed line; (c) *Panderodus* sp.: albid crown at oral tip, hyaline crown, and basal body that is bound internally by basal cavity (white dashed line) that extends from crown base. Panderodontid furrow extends from base to cusp tip. Scale bar = 0.2 mm.

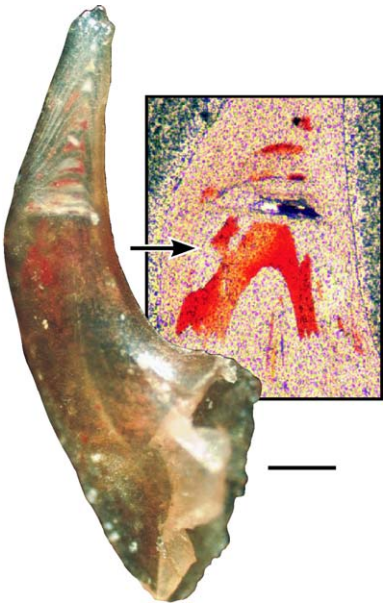

Fig. 2. Light microscope images of hyaline crown of the coniform element *Drepanoistodus suberectus* (Branson and Mehl) with longitudinal thin section (inset). Significant permeability is indicated by iron oxide precipitates within pores of lamellae and axial cavities. This specimen is unusual as it shows significant tissue damage and repair, which is marked by truncated lamellae midway along the cusp with subsequent growth comprising large axial cavities and oblique lamellae. FeO has been observed in many conodonts between lamellae and within axial cavities of hyaline crown. Scale bar = 0.2 mm.

mechanisms controlling marine trace element chemistry and subsequent diagenetic processes within subsea sediments has questioned the integrity of fossil bio-apatite geochemistry and the validity of earlier trace element geochemical data (Elderfield and Pagett, 1986; German and Elderfield, 1990; Toyoda and Tokonami, 1990). Consequently, post-depositional diagenetic masking of primary compositions is potentially a significant problem and the reliability of conodont apatite as a 'proxy' for palaeoseawater chemistry has yet to be demonstrated.

Our study attempts to shed light on some of these controversies and provide the foundations to better constrain the effects of diagenesis in order to discriminate [near] primary geochemical signatures from secondary overprinting. This demands spatially resolved compositional analysis of the target samples, as has been achieved by laser ablation ICPMS which provides the combined benefits of high spatial resolution and down-hole compositional depth profiling. The resultant compositional profiles are assessed in the context of histology and morphology to determine potential systematic trends, as well as their relative permeability, integrity, and susceptibility to diagenesis.

1.1. Bio-apatite chemical systematics and implications for palaeoseawater studies

The chemical structure of bio-apatites is fundamentally that of a carbonate-bearing calcium phosphate [$Ca_5(PO_4,CO_3)_3(F,OH)$] but can vary widely and contain impurities that can significantly effect its stability. Two structural Ca sites permit a diverse suite of cations to be substituted into the lattice (LeGeros, 1981), while anion substitution occurs at the OH (F, Cl, CO_3) and PO_4 (CO_3) sites. Bio-apatites are most commonly represented by carbonate hydroxyapatites (dahllite; e.g. bone), which stabilize to fluorapatite [$Ca_5(PO_4,)_3F$] over time by carbonate loss and fluorine uptake. However in seawater, the most thermodynamically stable species is the carbonate fluorapatite, 'francolite' (LeGeros, 1981; Jahnke, 1984), defined as having >1 wt.% of both F and CO_2 (McConnell, 1973). Francolite occurs in enameloids of fish teeth and scales and forms by a fluoride-concentrating mechanism during in-vivo mineralisation, with the content of F varying widely between taxa (LeGeros et al., 1978; LeGeros and Suga, 1980; Suga et al., 1980; LeGeros, 1981). In the case of bulk conodont crown, a non-stoichiometric chemical formula closest to francolite ($Ca_5Na_{0.14}(PO_4)_{3.01}(CO_3)_{0.016}F_{0.73}(H_2O)_{0.85}$) was determined by Pietzner et al. (1968), and various geochemical studies have identified >40 trace element cations incorporated within conodont mineralised tissues (Pietzner et al., 1968; Bradshaw et al., 1972; Wright et al., 1987a,b, 1990).

The minor and trace element contents of fossil bio-apatites are incorporated during in-vivo biologically-mediated growth, and subsequent postmortem diagenesis. Some minor elements (e.g. Sr) are incorporated in-vivo via substitution for major chemical components and thus have the potential to reflect original seawater conditions, provided the primary signature has not been significantly disturbed during diagenesis. In contrast, U, Th, and rare earth elements (REE) can become highly concentrated in biogenic apatites postmortem, with living phosphatic tissues containing only low trace levels of these elements, the REE within ppb ranges (Bernat, 1975; Wright et al., 1984; Shaw and Wasserburg, 1985; Trueman and Tuross, 2002; this study, e.g. Fig. 6). Moreover, the extremely low REE levels observed in extant species do not record a seawater composition due to biological mediation during phosphate mineralisation (Wright et al., 1984) and are prone to being overprinted immediately postmortem at or near the sediment–water interface (Bernat, 1975; Wright et al., 1984).

Various marine fossil bio-apatites have been used as proxies for palaeoseawater composition, especially as

recorders of apparent redox events in the geological record (e.g. Wright et al., 1984, 1987b). However, the complex processes driving REE fractionation at the sediment–water interface and within the pore waters of subsea sediments remain a significant issue for interpreting REE distribution patterns of fossil bio-apatites (Elderfield and Pagett, 1986; German and Elderfield, 1990; Reynard et al., 1999). Strontium, neodymium, oxygen, and carbon isotope systematics have also been a focus of earlier studies, the latter in extant marine faunas only (Vennemann et al., 2001). Although these isotope systems are commonly deemed to be robust, later diagenetic overprinting often occurs in highly permeable samples such as ichthyoliths (Elderfield and Pagett, 1986; Toyoda and Tokonami, 1990; Bertram et al., 1992). The reproducibility of conodont apatite data can also be an issue (Bertram et al., 1992; Cummins and Elderfield, 1994; Diener et al., 1996; Holmden et al., 1996; Trotter et al., 1999) and the significance of basal bodies as sources of chemical contamination has been demonstrated (Holmden et al., 1996; Trotter et al., 1999; Wenzel et al., 2000). However, the relative permeabilities and compositional differences between the two crown tissues of conodont apatite (albid and hyaline) has been overlooked, aside from two earlier studies suggesting differences in their calcium, phosphorus, sodium, carbonate, and organic contents (Pietzner et al., 1968; Wright et al., 1990). Increasingly sensitive microanalytical instrumentation now provide new opportunities to elucidate the chemical compositions of conodont histologies, and thereby constrain their inherent integrity and the effects of diagenesis.

It is important to emphasize that different mineralised tissues may have different susceptibilities to chemical modification during diagenesis. Their permeability and solubility is influenced by crystal size, ultrastructure, and composition. Vertebrate enamels, in particular, are often considered the most suitable candidates for geochemical analysis due to their dense crystalline structure, large crystal sizes hence smaller available surface area, and low organic contents. Yet despite their greater resistance to dissolution and diagenesis, enamels can become enriched in minor and trace elements (Kohn et al., 1999; Trueman and Tuross, 2002), and also exhibit isotopic modification due to postmortem uptake from the environment. Interpreting marine fossil bio-apatite geochemistry is further complicated by the lack of studies on extant faunas against which their true significance as geochemical proxies can be gauged. When using extinct fossil materials that lack modern equivalents, a broader appreciation of bio-apatite chemical systematics is important, and much caution is required as artefacts from secondary alteration cannot be constrained by comparative analysis with extant (primary) crystalline structures and compositions. In the case of conodont histologies, their primary character and integrity will always be uncertain.

2. Sampling and analytical techniques

2.1. Sampling

Well-preserved, thermally unaltered single conodont elements with a Colour Alteration Index (CAI) of 1 were selected for analysis. CAI is a measure of pyrolysis of the residual organics, an index of 1 indicating a burial temperature of <50 to 80 °C (Epstein et al., 1977). This eliminates the likelihood of diagenetic alteration from metamorphism but does not exclude the possibility of low temperature chemical exchange with diagenetic pore fluids.

From a collection of 590 bio-apatite specimens, 1140 compositional depth profiles of the component histologies were determined by laser ablation inductively coupled plasma mass spectrometry (LA-ICPMS). This database mainly comprises conodont analyses, supplemented by minor ichthyolith, inarticulate brachiopod, and modern marine fish data. Modern fish samples were caught from 4 different locations in the Pacific Ocean, including tropical waters off Queensland (Australia), and temperate waters off South Australia, New Zealand, southwestern Canada and northwestern USA. The fossil collections mainly derive from stratigraphic sections extending through the latest Cambrian–Ordovician–Early Silurian and a short interval spanning the Permo-Triassic boundary, representing 11 sites across 3 cratons, Laurentia, Australia, and South China, that are all within similar (sub)tropical palaeolatitudinal belts. The Early Palaeozoic samples are from Devon and Cornwallis islands of the Canadian Arctic Archipelago, Manitoba (Williston Basin), western Newfoundland, Manitoulin (southern Ontario) and Anticosti (Québec) islands in eastern Canada, the Canning (northwestern Australia), Amadeus (Northern Territory) and Georgina (Queensland) basins, while the Permo-Triassic boundary samples are from the GSSP Type section at Meishan, China. Holocene fish debris from high latitude marine sediment cores off Effingham Inlet (Vancouver Island) is also represented.

For brevity, the data figured herein were selected from 3 spatially and temporally disparate localities that represent the typical systematic trends determined from the larger dataset, which comprises both discrete temporal horizons and continuous stratigraphic sections (i.e. multiple populations). The figured data are from:

(1) Manitoba, which represents a discrete temporal horizon of Late Ordovician age from the Stony Mountain Formation; (2) Meishan, which includes multiple Late Permian samples from the Chanxing Formation; and (3) marine sediments off Vancouver Island, representing Mid–Late Holocene (5000–1000 BP) elasmobranch and hake remains.

Coeval conodonts and fish teeth were included in the Permian (Meishan) collection, and a suite of contemporaneous Silurian ichthyoliths (thelodont dermal scales), inarticulate brachiopods, and conodonts were further selected for comparative analysis, the latter derived from the Cape Phillips Formation, Devon Island (Sheills Peninsula), that range within the *Pterospathodus amorphognathoides* conodont biozone. Different biogenic apatites derived from the same rock matrix were specifically targeted to compare their relative compositions and uptake profiles. Several species of Holocene and modern fish scales, teeth, and bone were also analysed to compare recently fossilized and fresh marine bio-apatite compositions to help understand the diagenetic effects experienced by Palaeozoic ichthyolith and conodont apatite.

The Palaeozoic data figured represent samples from existing collections (C.R. Barnes, University of Victoria, Canada; R.S. Nicoll, Department of Earth and Marine Sciences, the Australian National University) that had previously been extracted from the carbonate host-rock by conventional acetic acid digestion and bromoform, tetrabromomethane, or sodium polytungstate heavy mineral separation techniques (Austin, 1987).

2.2. Laser ablation inductively coupled mass spectrometry (LA-ICPMS)

Compositional profiles through conodont elements, ichthyoliths, and modern fish skeletal components, have been measured in-situ by laser ablation ICPMS, using a custom-built laser sampling system interfaced between an ArF ($\lambda = 193$ nm) excimer laser (Lambda Physik LPX 120i) and quadrupole ICPMS (Agilent 7500s). A full description of the instrumentation used and its compositional depth profiling capabilities can be found in Eggins et al. (1998a,b, 2003) and details of instrument operating conditions are given in Table 1. Laser ablation ICPMS is ideally suited for analysing conodonts due to the ability to measure compositional variations within single conodont elements. More specifically, it has the capability to determine with high spatial resolution, continuous compositional depth profiles through the concentric layered structure of the component histologies (Fig. 1). In this regard, it should be noted that the ANU (RSES) laser ablation system produces flat bottomed ablation pits and incorporates a unique sample cell design that produces a rapid signal response to any change in ablated composition (time for decay to 10% of peak signal intensity is ~1.3 s for all elements). Collectively, these features facilitate very high spatial resolution continuous depth profiling when performing conventional spot analysis (Eggins et al., 2004). Optimum (sub-micron) depth resolution is obtained where ablation pit aspect ratios (depth/diameter) are less than 1, and degrades with increasing pit depth due to sampling of material from pit sidewalls and the development of topography on the ablation pit base (see Eggins et al., 1998b).

Conodont elements were washed in Milli-Q water, affixed to double-sided adhesive carbon tape attached to a glass slide, and placed within the sample cell. Compositional depth profiles that pass completely through individual conodont elements were determined by continuous sampling using a 5 Hz laser pulse rate and fluence of 8 J/cm^2. The ablation rate for biogenic apatite is estimated to be ~1 μm/s, based on a measured ablation depth per pulse of ~0.2 μm in inorganic (Durango) apatite. Different parts of conodont elements, including specific histologies, were targeted for analysis using laser spot diameters of 40, 48, or 65 μm.

Table 1
Laser ablation and ICPMS operating conditions

ICPMS: Agilent 7500s		**Laser: Lambda Physik LPX120i**	
Forward power	1200 W	Pulse rate	5 Hz
Carrier gas	5 cm^3/s He 20 cm^3/s Ar	Fluence Power density	8 J/cm^2 0.3 GW/cm^2
Sampling depth	6.5 mm	Ablation medium	He
ThO^+/Th^+	<0.5%	Wavelength	193 nm (ArF)
$^{232}Th^+/^{238}U^+$	>0.9 for NIST612	Beam diameter	40, 48 or 65 μm
Detector (ETP DDEM)	Simultaneous pulse counting & analogue	Objective lens	f=125 mm (coated doublet)

More than 40 elements (typically including Li, B, Na, Mg, Al, Si, K, Ca, Sc, Ti, V, Mn, Fe, Ni, Zn, As, Rb, Sr, Y, Zr, Cd, Sb, Cs, Ba, REE (La to Lu), Hf, Pb, Th and U) were profiled during each analysis. Data collection was performed by rapid peak-hopping (20 or 30 ms dwell times, for a total mass cycle time of ~1 s) between selected isotopes of each analyte element for a period of 150 or 200 s. Data reduction followed the method outlined by Longerich et al. (1996), using mean background corrected intensities and ^{43}Ca as the internal standard to correct for variation in mass ablation yield based on a conodont apatite CaO concentration of 53 wt.% (average reported by Pietzner et al., 1968, and measured by electron microprobe during this study). The international glass reference material NIST612 was used for external calibration, employing the preferred concentrations reported by Pearce et al. (1997). Details of the measured isotopes, NIST612 calibration values, and detection limits are listed in Table 2. The mean and standard deviation of repeat analyses of a matrix-

Table 2
Analysed elements and isotopes, NIST612 values, and results obtained for Durango apatite

Element (ppm/*wt.%)	Isotope (amu)	NIST612	DL (t=20 s)	Durango soln-ICPMS	Durango LA-ICPMS	Std. dev. (n=30)	%RSD
B	11	33.7	0.45	nd	13.0	4.6	36
Na_2O*	23	13.96	0.0003	nd	nd	–	–
Mg	24	78	0.34	nd	202.3	5.4	2.7
Al_2O_3*	27	2.10	0.00013	nd	<0.00013	–	–
SiO_2*	29	71.79	0.08	nd	0.22	0.02	10.2
CaO*	43	11.91	0.009	nd	56.0	–	–
Sc	45	41.0	0.09	<3	0.13	0.03	21.4
Ti	49	48.5	1.0	<5	<1.0	–	–
V	51	38.2	0.07	30.2	28.7	0.4	1.3
Mn	55	38.5	0.15	92.4	92.0	0.8	0.9
Fe	57	55.6	6.9	nd	326	9	2.7
Ni	60	37.8	0.17	<14	0.47	0.25	53.1
Zn	66	36.6	0.12	<1.3	<0.12	–	–
As	75	37.3	0.29	nd	802	23	2.9
Rb	85	31.6	0.05	0.17	0.06	0.01	15.8
Sr	86	76.4	0.48	462	475	11	2.2
Y	89	37.8	0.010	560	456	13	2.9
Zr	90	36.0	0.035	1.0	0.51	0.02	4.3
Cd	111	28.0	0.12	nd	<0.12	–	–
Sb	121	38.4	0.10	nd	<0.1	–	–
Cs	133	41.6	0.07	0.002	<0.07	–	–
Ba	137	38.5	0.045	1.72	1.44	0.06	4.3
La	139	35.5	0.008	3540	3370	87	2.6
Ce	140	38.2	0.008	4660	4282	116	2.7
Pr	141	37.1	0.008	374	336	9	2.8
Nd	146	35.0	0.034	1080	1040	29	2.8
Sm	147	36.4	0.018	136.7	126.9	3.3	2.6
Eu	153	34.6	0.010	14.0	15.34	0.43	2.8
Gd	158	37.1	0.019	112.2	109.2	3.2	2.9
Tb	159	36.3	0.008	14.6	12.87	0.42	3.3
Dy	163	35.7	0.028	72.6	73.9	3.0	4.0
Ho	165	37.9	0.007	14.8	14.28	0.51	3.6
Er	166	38.0	0.016	40.3	38.6	1.3	3.4
Tm	169	37.7	0.006	nd	4.85	0.21	4.3
Yb	174	39.5	0.018	28.0	27.8	0.9	3.3
Lu	175	37.6	0.007	3.86	3.65	0.13	3.7
Pb	208	38.7	0.04	0.58	0.53	0.03	4.8
Th	232	37.3	0.009	192.4	181.3	8.6	4.8
U	238	36.9	0.009	9.09	8.88	0.37	4.1

Detection limit (DL) values are based on typical background variance and analyses sensitivity when analysing NIST612 glass using a 48 μm spot diameter and integration time of 20 s. These DL values will vary (decrease/increase) with the square of the integration time and spot diameter used. NIST612 values are from Pearce et al. (1997). SiO_2, Al_2O_3, CaO and Na_2O concentrations are reported in wt.% and 'nd' indicates element not determined. Durango apatite reference values have been measured by solution ICPMS following the method of Eggins et al. (1997). %RSD values indicate the long-term (run-to-run) reproducibility of measured trace element concentrations in Durango apatite.

matched (Durango apatite), in-house standard indicate the analytical reproducibility over the course of this study was in the range 1–5% (see Table 2). The accuracy of our LA-ICPMS technique for the analysis of conodonts and other biogenic or inorganic apatites is further indicated by the close agreement between results obtained for the Durango apatite and determinations made by solution ICPMS (typically <5–10% difference with the exception of Y; see Table 2).

Multiple analyses of each specimen were undertaken to monitor changes in composition along the growth axis and within different tissues of the same specimen. The larger diameter spot sizes were employed for analysis of thicker conodont elements to minimize the effects of inter-element fractionation when sampling from large aspect ratio pits (Eggins et al., 1998b). Experiments made using Durango apatite indicate that inter-element fractionation with respect to the internal standard (Ca) is small (<5–10%) where ablation pit aspect ratios (depth/diameter) are <4, and similar to that observed in NIST612 glass for the majority of elements that are of primary interest to this study (i.e. REE, V, Mn, Fe, Y, Mg, Sr, Ba, Th and U). Large fractionations occur only in the case of B, As, and Pb, for which measured concentrations increase steadily with ablation pit depth, and reach apparent values that are 30–40% higher for ablation pit aspect ratios between 3 and 4.

2.3. Fourier transform infrared spectroscopy (FTIR)

Fourier Transform Infrared Spectroscopy of conodont histologies was performed on a Bruker IFS28 infrared spectrometer, coupled to a Bruker A590 infrared microscope. Spectra were determined directly from ion-milled thin sections of conodont elements, which had been prepared for TEM analysis. The infrared beam (~50 μm) was focused on the thin section and multiple spectra from different spots across conodont basal body, hyaline, and albid crown tissues of "*Cordylodus robustus*" and *Plectodina*? sp. were recorded within the range of 600 to 6000 cm^{-1}.

3. Results

LA-ICPMS profiles reveal significant compositional variability within conodont mineralised tissues, with large systematic differences occurring for the rare earth elements (La–Lu) and Y, and occasionally for Pb, Th, and U (see Section 3.1.1). These particular elements, which are largely incorporated postmortem (see Section 4), form the most striking compositional trends and are the principle focus of this paper. Furthermore, enrichments and depletions at the growth axis are shown to be influenced by morphological structure (see Section 3.1), whereas the elevated concentrations of many elements at the conodont margins may partly be due to residual surface contaminants. Mg and Sr moreso have high concentrations often with significant variability independent of tissue type, aside from the typically lower Sr concentrations in conodont basal bodies (see Section 3.2). Si, Al, Sc, Ti, Rb, Sb, and Cs typically have very low concentrations generally near background levels, and most other elements show no systematic compositional variation.

It should be noted that several representative conodont samples were also analysed by electron microprobe to confirm major and minor element (Na, Ca, P, F) compositions reported within the literature. These data proved to be consistent with compositions reported earlier (Pietzner et al., 1968; Wright et al., 1990), particularly the higher P but lower Na contents of albid compared to hyaline crown.

3.1. Systematic compositional trends

3.1.1. Conodonts

The systematic compositional differences in Y and REE contents between the two crown tissues, as well as the large and highly correlated variations of these elements, are particularly distinctive. These chemical systematics are clearly illustrated by differences in the mean concentrations of Y and REE analysed in conodonts from Manitoba (Fig. 3). In contrast, other elements do not exhibit compositional trends that are consistent between localities and thereby most likely reflect local environmental conditions. The structure of LA-ICPMS profiles also reflects these systematic compositional variations between the component histologies. Albid tissue is characterised by ∪-shaped profiles with axial depletions (Fig. 4d,g,k) up to several orders of magnitude. This contrasts with the enriched and typically homogeneous profiles of hyaline tissue (Fig. 5) that show variable depletions or enrichments (Fig. 4e,h) at the growth axis. These distinct profiles have significant implications for the relative permeability and diagenetic susceptibility of these histologies (see Section 4), as is further indicated by significant enrichments coincident with the panderodontid furrow in the albid profile of Fig. 4k.

To facilitate comparison of the different samples, mean elemental concentrations were calculated for several zones within each profile, including an axial and intermediate interval between the conodont margin

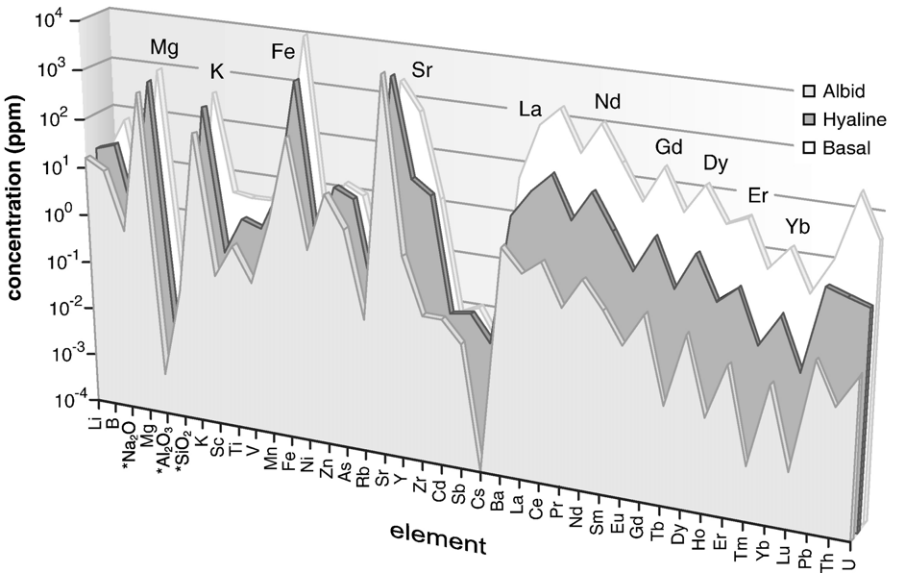

Fig. 3. Mean (axial) concentrations of elements analysed in conodonts from Manitoba (Late Ordovician) showing large differences in Y and REE contents of the component histologies typical of all sample localities. Note that concentrations are in ppm with the exception of Na_2O, SiO_2, and Al_2O_3 that represent wt.% values.

and axis (Fig. 5). For brevity, all concentrations quoted herein are those calculated from the axial interval, and it should be noted that the growth axis may not be centrally located as it relates to the symmetry of the specimen. Axial intervals are typically recognised by the presence of Sr minima in either crown tissue, and REE minima in albid crown or REE depletion/enrichment spikes in hyaline tissue profiles (Figs. 4 and 5). The ensuing discussion of compositional ranges and trends draws upon the collective dataset of spatially disparate localities represented by both continuous stratigraphic sections and discrete temporal horizons (see Section 2.1).

The relative concentrations of Y and REE in albid, hyaline, and basal body tissues range over many orders of magnitude (Fig. 6b,c,e,f), with Y, LREE (represented by La), and MREE (represented by Nd) concentrations typically less than 10 ppm to below detection limits in albid tissue, between 10 and 100 ppm or more (up to ~500 ppm for Y) in hyaline crown, and up to ~1000 ppm in basal bodies. HREE (represented by Yb) follow a similar pattern of variation but with overall lower concentration levels than LREE and MREE. U and Pb can also show a large range in concentrations and in two of the three samples representing discrete temporal horizons (Manitoba and Manitoulin Island), show a linear correlation within hyaline and basal conodont tissues (e.g. Fig. 6o). These elements are usually <1 ppm in albid tissue, up to 10 ppm or more in hyaline crown, and between 10 and 100 ppm in basal tissues. Th concentrations also increase from <1 ppm in albid tissue up to ~100 ppm in hyaline crown, and reach ~1000 ppm in basal tissues (Fig. 6l) .

Deviations from the distinctive ∪-shaped concentration profiles of albid tissue appear to be linked with sample opacity, which can vary widely between and within specific taxa. Opacity is determined by pore size, which may be variably developed in all crown tissues (Trotter et al., submitted for publication), and is not exclusive to albid crown with cancellate porosity. Tissue commonly referred to as albid, often 'incipiently' developed, has been shown to have a lamellar structure (Donoghue, 1998; Trotter et al., submitted for publication) and further complexity in the crystalline structure of albid crown has been recently revealed by TEM imaging (Trotter et al., submitted for publication). These variants in albid crown ultrastructure expose the ineffectiveness of light microscopy for discriminating specific crown histologies, and may further account for the apparent overlap in element concentrations between albid and hyaline tissues.

Aside from Sr (Fig. 6h,i), conodont basal bodies are highly enriched in most elements compared to crown tissues, being more enriched than hyaline crown by up to several orders of magnitude (Figs. 4l and 6c,f,l,o). The density of basal tissue mineralisation may also be variable and thereby affect the uniformity of the compositional profile. Basal cavities of specimens in which the basal body has not been preserved show enriched profiles that may reflect compositions of remnant basal tissue and/or secondary detrital

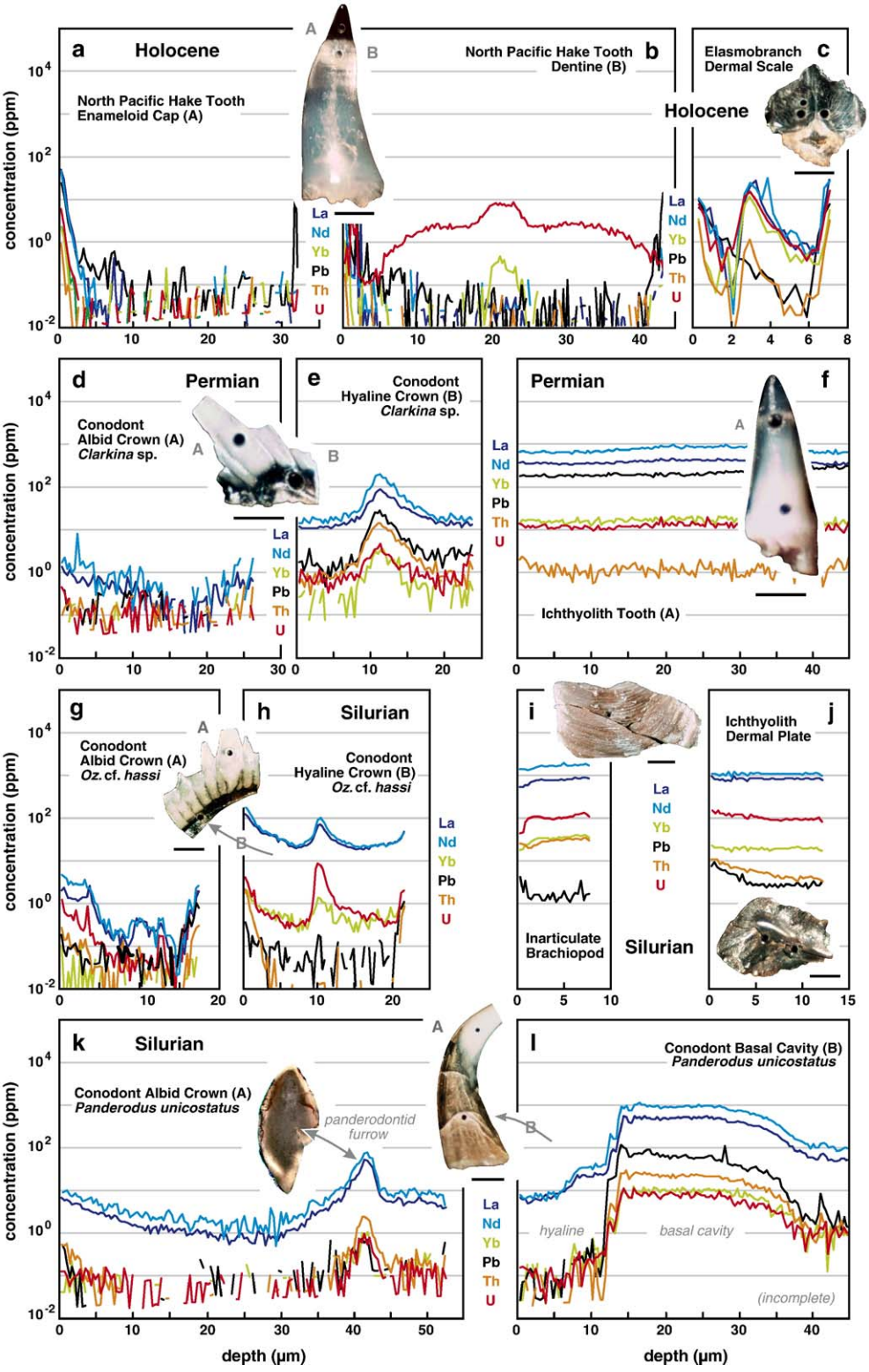
a Holocene
North Pacific Hake Tooth Enameloid Cap (A)
b
North Pacific Hake Tooth Dentine (B)
c
Elasmobranch Dermal Scale
Holocene
d Permian
Conodont Albid Crown (A) Clarkina sp.
e
Conodont Hyaline Crown (B) Clarkina sp.
Permian
f
Ichthyolith Tooth (A)
g
Conodont Albid Crown (A) Oz. cf. hassi
h Silurian
Conodont Hyaline Crown (B) Oz. cf. hassi
i
Inarticulate Brachiopod
Silurian
j
Ichthyolith Dermal Plate
k Silurian
Conodont Albid Crown (A) Panderodus unicostatus
panderodontid furrow
l
Conodont Basal Cavity (B) Panderodus unicostatus
hyaline
basal cavity
(incomplete)
La
Nd
Yb
Pb
Th
U
concentration (ppm)
depth (μm)

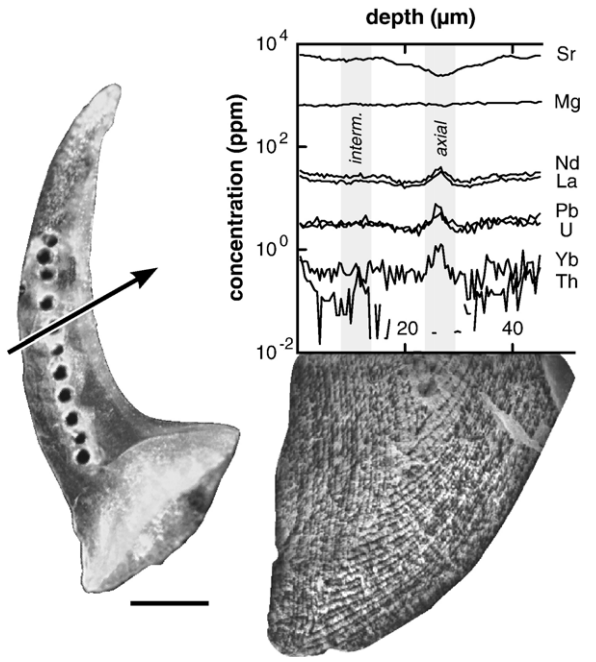

Fig. 5. LA-ICPMS profile of selected chemical species through hyaline crown of *Drepanoistodus suberectus* (Branson and Mehl). The profile structure is essentially homogeneous suggesting equilibration with diagenetic pore fluids, with the exception of slight axial enrichments in REE, Pb and U and depletion of Sr. SEM image of the transverse section adjacent to the ablation pit (arrow) shows the depletion/enrichments correlate with the growth axis. Axial and intermediate intervals from which concentrations are calculated are shown. Scale bar = 0.2 mm.

contaminants contained within the cavities. This is also shown in Fig. 4l by the sharply stepped transition in compositions between the outer hyaline tissue and basal cavity, which likely contains remnant basal tissue.

3.1.2. Fish remains and inarticulate brachiopods

Chemical profiles of a selection of Late Permian and Early Silurian ichthyoliths (fish teeth and scales) and phosphatic inarticulate brachiopods are compared to those of conodont crown tissues from the same rock samples (Fig. 4d–j). These show typically uniform, enriched profiles of many elements, especially Y, REE, Pb, and U that are akin to the profiles of hyaline conodont crown and basal tissues. Pb, Th, and U concentrations in ichthyolith and brachiopod apatite generally fall between 10 and 100 ppm, with Y, LREE (e.g. La), and MREE (e.g. Nd) concentrations ranging from 100 to >1000 ppm (Fig. 7) whereas HREE (e.g. Yb) are considerably lower (<20 ppm).

Compositional profiles of Holocene ichthyoliths usually show low trace element concentrations, often below detection limits (Fig. 4a–b), with Pb and Th typically <1 ppm (Fig. 6j,m), and U and REE between 0.01 and ~10 ppm (Figs. 4b,c and 6a,d,m). However, some profile intervals show more enriched zones (>1 ppm) of Y and REE (Fig. 4c), which likely coincide with regions of greater permeability (e.g. vascular canals and pulp cavities; Fig. 4b–c) that can facilitate postmortem uptake of these elements. Rare earth element and Th concentrations of modern fish bones, teeth, and scales are typically below detection limits, yielding depth profiles similar to the enameloid cap of the Holocene hake tooth (Fig. 4a). Y concentrations are also very low (≤0.01 ppm) compared to fossil bio-apatites, whereas U and Pb may range to 1 ppm. Sr concentrations essentially range between 500 and ~3000 ppm, and are shown for comparison with fossil bio-apatites (Figs. 6g–i and 7c,d).

3.1.3. Element correlations in fossil bio-apatites

The similarity in geochemical behaviours of Y and REE is manifested as strong positive linear correlations within and between the various histologies from all sample localities. These correlations consistently show albid crown having the lower concentrations, whereas hyaline compositions are intermediate between albid crown and the high concentrations of basal body, ichthyolith, and inarticulate brachiopod apatites. Weaker correlations also occur between Pb–Th–U but are not consistent between localities, possibly reflecting local influences, such as burial history and pore water chemistry. The Pb, Th, and U datasets for Manitoba show distinct offset clusters for the component tissues (Fig. 6l,o), compared to the more common 'shotgun scatter' observed in other localities. Similar correlated and/or clustered patterns occur within the two other Ordovician samples (Newfoundland and Manitoulin Island) that also represent discrete temporal horizons.

Inter-element correlations have been systematically assessed for 6 sampling localities that provided large

Fig. 4. Representative LA-ICPMS compositional profiles of selected chemical species through various histologies of fossil bio-apatites: Holocene ichthyoliths from core Tul099B03 (a–c); Permian conodont albid (d) and hyaline crown (e) of *Clarkina* sp., and coeval ichthyolith (f) from sample DC-9; Silurian conodont albid (g) and hyaline crown (h) of *Ozarkodina* cf. *O. hassi* (Pollock, Rexroad and Nicoll), and coeval inarticulate brachiopod (i) and ichthyolith (j) from sample #489; and Silurian conodont albid tissue (k) with subsequent transverse section through cusp at ablation pit 'A' showing panderodontid furrow (inset), and basal cavity (l) of *Panderodus unicostatus* (Branson and Mehl) from sample #478. Scale bars for (a–c), (g–l) = 0.2 mm, and (d–f) = 0.1 mm. Note—breakage of some specimens occurred after ablation.

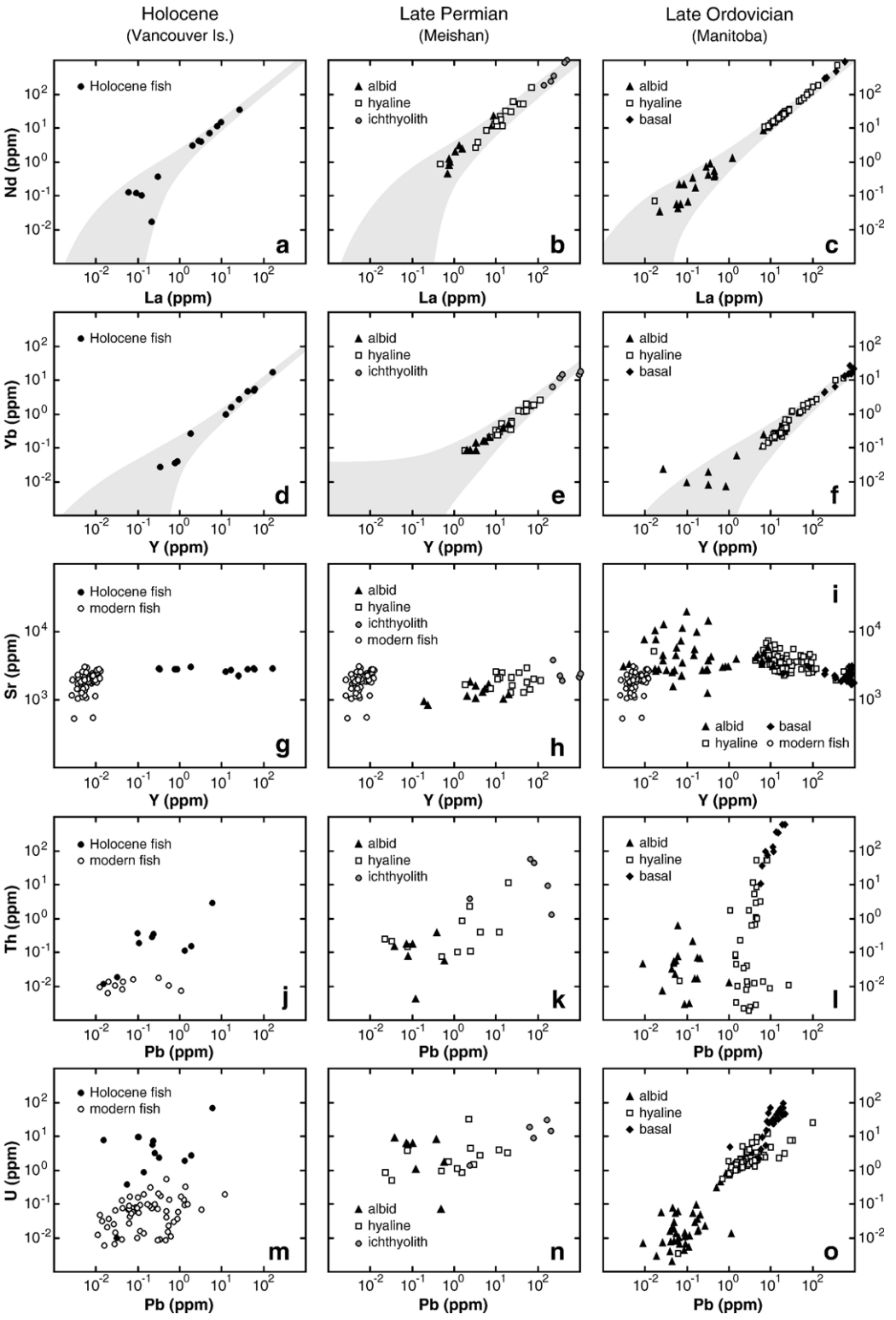
Holocene
(Vancouver Is.)
Late Permian
(Meishan)
Late Ordovician
(Manitoba)
Holocene fish
albid
hyaline
ichthyolith
basal
modern fish
Nd (ppm)
Yb (ppm)
Sr (ppm)
Th (ppm)
U (ppm)
La (ppm)
Y (ppm)
Pb (ppm)
a
b
c
d
e
f
g
h
i
j
k
l
m
n
o

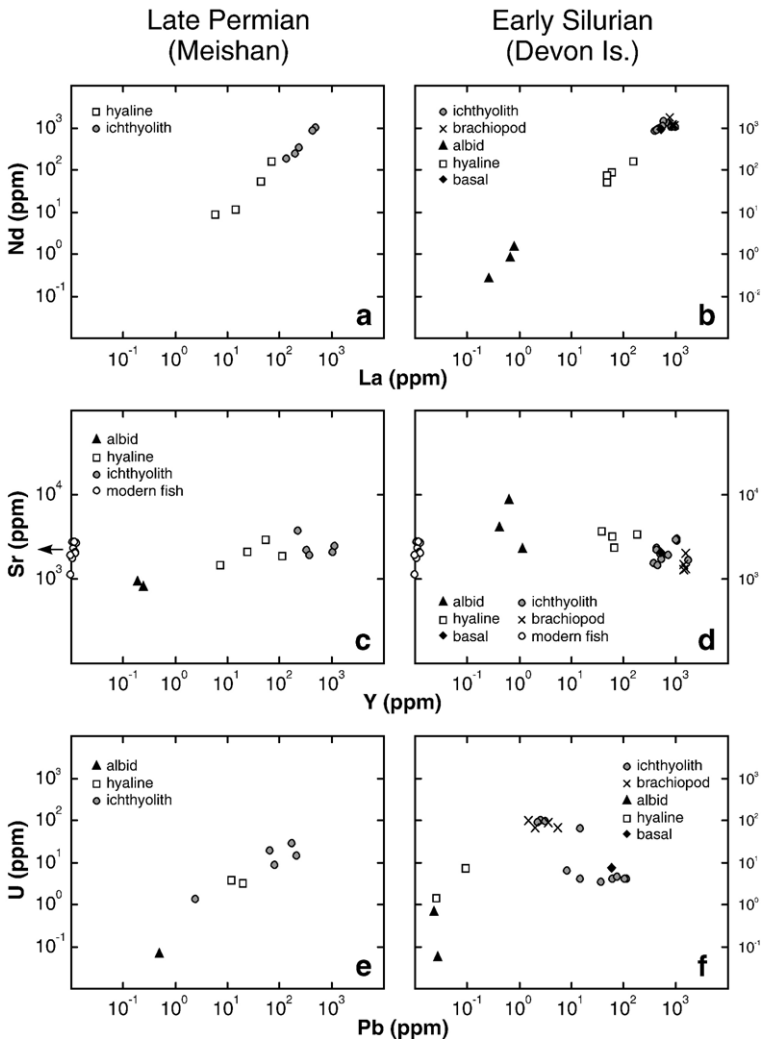

Fig. 7. Comparative plots for La–Nd (a–b), Y–Sr (c–d), and Pb–U (e–f) concentrations within contemporaneous conodont, ichthyolith, and inarticulate brachiopod apatites from Late Permian (Meishan) and Early Silurian (Sheills Peninsula, Devon Island) samples. Note change in scale compared to Fig. 6 in order to include higher concentration ranges.

datasets, specifically the 3 samples representing discrete temporal horizons from Newfoundland (Mid Ordovician), Manitoba (Late Ordovician), and Manitoulin Island (Late Ordovician), as well as 3 localities comprising continuous stratigraphic sections from Devon (Ordovician), Cornwallis (Early Silurian), and Anticosti (Early Silurian) islands. Pearson Product-Moment Correlations were determined for conodont crown tissues and Holocene ichthyoliths, there being too few data for a robust statistical analysis of conodont basal tissue, and Palaeozoic ichthyolith and brachiopod material. Aside from Y–REE, correlations with Ba (Ba–Y–REE) were found to be common in hyaline conodont tissues for 5 of the 6 localities. Additional correlations were also observed between some other trace elements, including Mn, Fe, As, Zr, Al, and Sc, in at least 2 localities and in some cases these correlate with Pb, Th, and U. Collectively, these varied correlations suggest

Fig. 6. Ranges in concentrations for La–Nd (a–c), Y–Yb (d–f), Y–Sr (g–i), Pb–Th (j–l) and Pb–U (m–o) within the various histologies of conodont, ichthyolith, and inarticulate brachiopod apatites from the 3 representative localities of Holocene (Vancouver Island), Permian (Meishan) and Late Ordovician (Manitoba) ages. Note that ranges in concentrations for Y–Sr of modern fish form a tight cluster that is compared with all 3 fossil sample suites, while Pb–Th and Pb–U ranges are plotted with Late Holocene fish samples, which show postmortem enrichment. Shaded areas (a–f) represent 95% confidence bands for linear regressions weighted using analysis uncertainties. The two highest concentrations points in (e) are excluded from the regression.

that hyaline crown may incorporate a broad range of elements from pore waters during diagenesis, whereas uptake by albid crown is limited to considerably lower concentrations of Y–REE, and occasionally Pb, Th, and U.

There is no apparent correlation between Sr and Y–REE (Figs. 6i and 7d), Pb, Th, or U within the collections analysed, apart from a subtle positive trend in the Permian samples (Fig. 6h). Since modern fish REE contents are below detection limits of LA-ICPMS analysis, Y is used as an analogue for REE to facilitate comparison of modern and fossil data.

Weighted linear regressions of Y–REE data presented in Fig. 6 (weighting based on analytical uncertainties) produce tight linear fits that are consistent with simple mixing of two components (Fig. 6a–f). However, the low Y–REE (albid) end of the regression lines is quite poorly constrained as indicated by the increasing relative width of the 95% confidence bands. This unfortunately precludes any firm constraints being placed on the albid end-member composition, or the possibility of estimating a hypothetical primary conodont apatite composition by regression extrapolation to very low REE and Y concentrations (i.e. to Y concentrations within the range of modern fish, Fig. 6g).

3.1.4. Shale-normalised REE abundance patterns in fossil bio-apatites

REE concentrations for all analysed samples were normalised to the modified PAAS values of McLennan (1989). Although some variations occur between localities, the typical MREE enriched (convex) pattern documented by previous conodont studies is most common, as shown by the Late Permian and Early Silurian conodont, ichthyolith, and brachiopod samples (Fig. 8) depicted previously in Fig. 4. The Holocene elasmobranch dermal scale also depicted in Fig. 4c, gives an enriched modern seawater-like pattern that lacks a negative Ce anomaly (Fig. 8b). Conodont basal tissue, ichthyolith, and brachiopod apatite have similar convex patterns with high levels of enrichment whereas hyaline tissues and some (apparent) albid samples yield similar REE patterns but at lower abundance levels. However, many albid crown samples have extremely low concentrations that fall below detection limits, which preclude assessment of their shale-normalised REE abundance patterns.

3.2. Non-systematic compositional variations

Sr and Mg behaviours are briefly described below given their general importance in palaeoceanography and relatively high concentrations in conodont apatite. Both Sr and Mg are substantial constituents of seawater, in which they have long residence times, and their ratios to Ca (i.e. Mg/Ca and Sr/Ca ratios) in biogenic carbonates have been widely recognised as proxies for palaeoseawater temperature. Since Sr and Mg are incorporated in-vivo by biogenic apatites via substitution for Ca, their abundances (or equivalent ratios to Ca

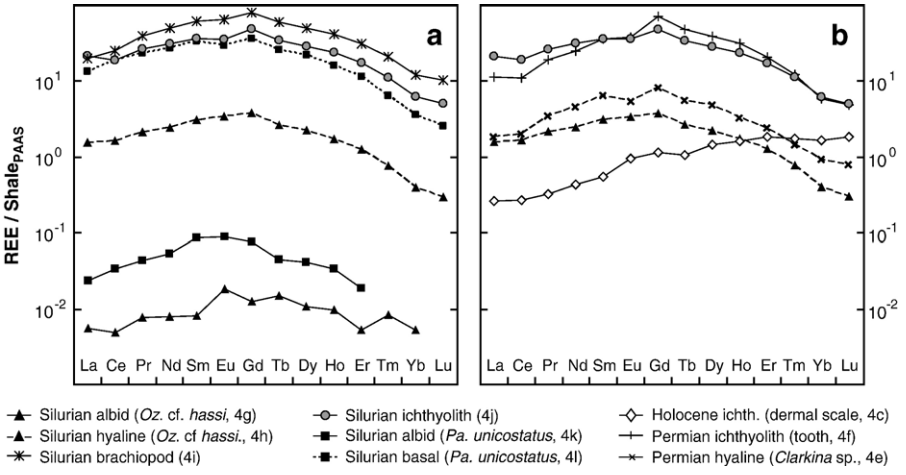

Fig. 8. Shale-normalised (PAAS) REE abundance patterns are shown for the axial concentrations of the representative samples depicted in Fig. 4, as denoted by bracketed numbers: (a) Early Silurian conodonts (*Ozarkodina* cf. *O. hassi* and *P. unicostatus*), albid crown, hyaline crown, and basal tissue/cavity, inarticulate brachiopod valve, and ichthyolith; (b) comparison of Late Permian (*Clarkina* sp.) and Early Silurian conodont (*Ozarkodina* cf. *O. Hassi*), hyaline crown from (a), with Late Permian, Early Silurian and Holocene ichthyoliths. PAAS values taken from McLennan (1989): 38.2 (La), 79.6 (Ce), 8.83 (Pr), 33.9 (Nd), 5.55 (Sm), 1.08 (Eu), 4.66 (Gd), 0.774 (Tb), 4.68 (Dy), 0.991 (Ho), 2.85 (Er), 0.405 (Tm), 2.82 (Yb), 0.433 (Lu).

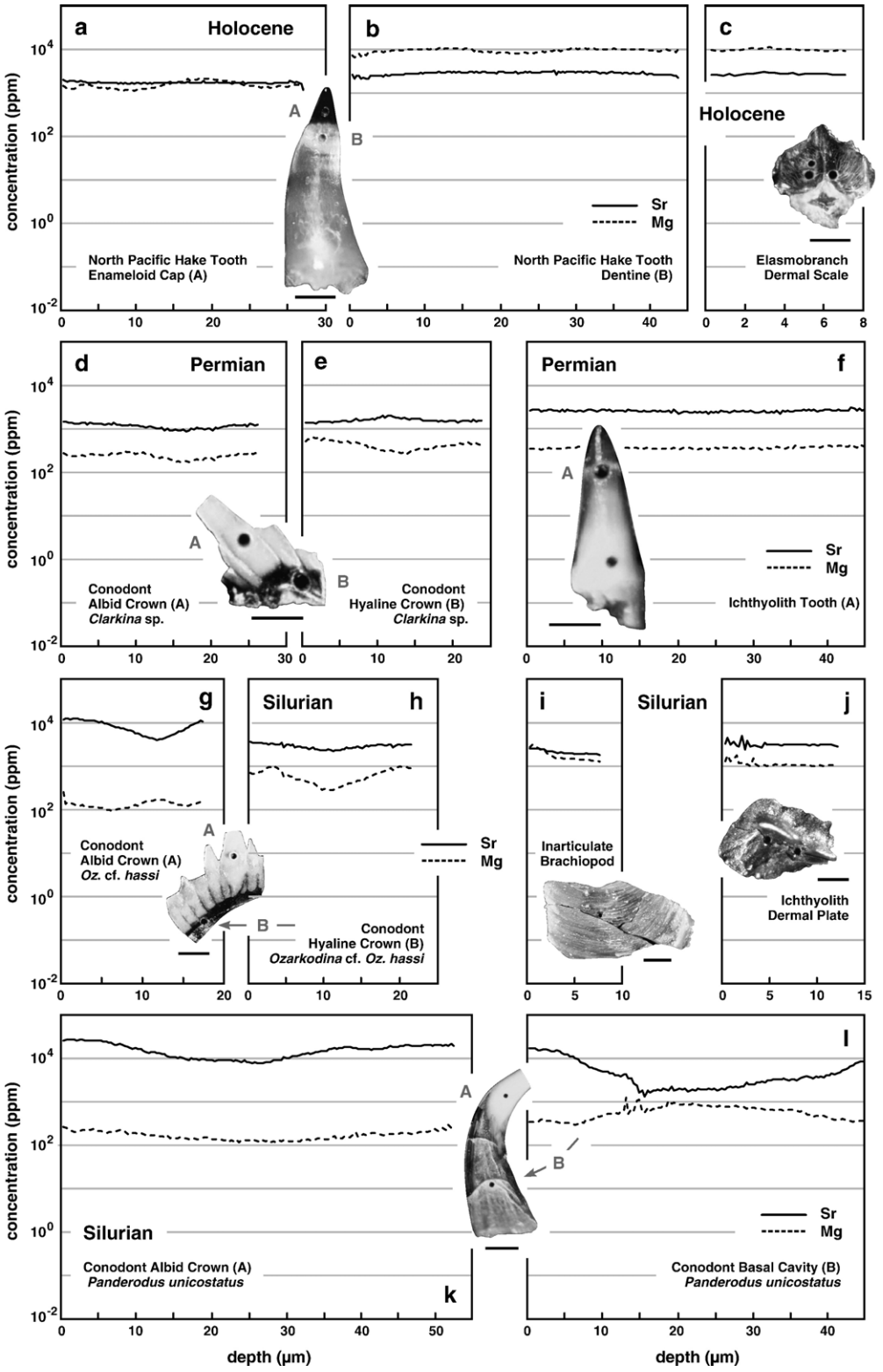

Fig. 9. Representative LA-ICPMS compositional profiles of Sr and Mg through various histologies of fossil bio-apatites, which are also shown in Fig. 4.

obtained by multiplication using appropriate atomic weight ratio conversion factors) also hold some potential as environmental proxies, as is the case for Sr isotopes. However, identifying new environmental proxies using elements with variable and non-systematic behaviours requires careful assessment of in-vivo and postmortem processes, with the systematic analysis and comparison of fossil and modern marine samples.

Conodont Sr concentrations are high and variable (Fig. 9), ranging from levels similar to and slightly higher than modern fish apatite (1000–3000 ppm, see Fig. 6g). Basal body tissues typically have lower Sr contents of several 1000 ppm compared to crown tissues that often range to tens of thousands ppm, as reported previously (Pietzner et al., 1968; Holmden et al., 1996). Sr appears to behave similarly in both hyaline and albid crown, and has fairly uniform to more typically concave profiles with slight to moderate axial depletions (Figs. 5 and 9). Sr is not correlated systematically with any other element including REE which are adsorbed postmortem, suggesting primary Sr signatures may not be strongly overprinted by postmortem uptake events. Earlier work has shown distinct decreases in $^{87}Sr/^{86}Sr$ isotopic compositions toward the 'core' of individual conodont elements (Trotter et al., 1999; Trotter, unpub. data), consistent with the axial depletions observed in LA-ICPMS profiles representing zones of lesser or minimal secondary overprinting. In contrast, elevated Sr concentrations in fossil ichthyoliths (compared to living fish), and Sr isotope compositions that are offset from the seawater evolution curve toward pore water compositions, show evidence of limited Sr uptake during early diagenesis (Martin and Scher, 2004). However, such effects are likely influenced by the crystalline properties and ultrastructure (i.e. permeability) of the host sample, which clearly varies between taxonomic groups and their component histologies.

No systematic differences in Mg composition have been observed between conodont tissue types. Concentrations are typically 100's ppm but may range to several 1000's ppm, often with uniform to convex profiles that are significantly more variable than Sr (Figs. 5 and 9). Mg/Ca ratios in hyaline crown typically show much greater dispersion and poor reproducibility compared to albid tissue, suggesting hyaline tissue may be more susceptible to chemical overprinting. However, any firm conclusion is hampered by the difficulties in discriminating 'true' albid crown by light microscopy, and the unknown behaviour of Mg/Ca in modern biogenic apatites. As with the many other elements that also vary within and between samples but lack distinctive systematic trends, the significance of Sr and Mg contents remains unclear and will be the subject of further study.

4. Discussion

Analyses of inarticulate brachiopods, ichthyoliths, and conodonts from the same samples, as well as those of younger Holocene and modern fish remains, have provided insights into the chemical systematics of marine biogenic apatite, and their relative integrity and potential as geochemical tracers, particularly within the context of post-depositional modification. The contrast in trace element geochemistry between the two conodont crown tissues is significant because it pertains to elements that are known to be strongly adsorbed by biogenic apatites postmortem (e.g. REE, Y, Th, and U; Bernat, 1975; Wright et al., 1984; Millard and Hedges, 1996; Kohn et al., 1999; Trueman and Tuross, 2002; Eggins et al., 2003). The rates and extent of postmortem trace element uptake is greatly influenced by histological structure and consequent permeability, as well as available crystal surface area of the host tissue, which is reflected by the contrasting LA-ICPMS compositional profiles of the conodont crown tissues.

The trace element geochemistry of biogenic apatite is strongly influenced by postmortem uptake in the case of Y and REE, whereas other elements may display more complex behaviours due to their variable incorporation via both in-vivo and postmortem processes. Variability in element incorporation during biomineralisation, especially in the context of external environmental controls, is poorly constrained even within the modern marine biogenic phosphate system. Faced with this fundamental unknown, further discussion is limited to chemical species that show distinctive systematic trends within and between the various tissues analysed, essentially their Y, REE, and heavy element compositions that have been derived postmortem.

4.1. Postmortem chemical exchange and sample permeability

Models of post-depositional U-uptake via diffusion–adsorption processes in archaeological bone and teeth provide a framework for understanding the uptake of U and other trace elements by bio-apatites. Zones of low concentration reflected by the interior of ∪-shaped profiles likely represent the least altered, and potentially, the primary biomineralised composition (Millard and Hedges 1996; Pike and Hedges, 2001; Eggins et al., 2003). Accordingly, elevated concentrations at the margins of conodont albid tissue could reflect surface

contamination and/or restricted uptake into the outer zones of the tissue. This interpretation is supported by the low to below detection limit concentrations of rare earth and heavy elements (Pb, Th, U) in LA-ICPMS profiles of the enameloid caps of some Holocene (Fig. 4a) fish teeth and in modern fish apatite. Leaching during later diagenetic events is discounted in the case of ∪-shaped albid profiles as modelling suggests element desorption and loss from the sample produces lower concentrations at the margins, resulting in M- or ∩-shaped profiles, and ultimately equilibration to uniform profiles at lower concentration levels. Importantly, such leaching effects would be expected in adjacent hyaline tissue but have not been observed.

Variably developed axial depletions (¬⌄¬) and enrichments (_∧_) within hyaline tissue have been observed for a number of elements (e.g. Fe, Mn, Al, Zn) and are interpreted to reflect the contents of the axial growth cavities in which secondary precipitates may reside (Fig. 2). These axial enrichments/depletions may range up to several orders of magnitude and thus potentially bias analyses derived from bulk conodont samples. Similar enrichments characterise highly permeable basal tissues and may also occur in panderodontids, where the longitudinal furrow acts as a conduit for fluid ingress and element transport (Fig. 4k). Likewise, basal cavities are likely a major source of contamination after postmortem loss of the basal body as they provide a reservoir for the accumulation of detritus. Accordingly, all basal components (basal bodies and cavities) should be excluded from geochemical studies, with crown tissues the prime target and specifically albid crown where original biomineralised compositions are sought.

In contrast to albid crown, basal and hyaline tissues are characterised by much higher elemental concentrations and comparatively uniform compositional profiles (Fig. 5), which is attributed to their greater adsorption (i.e. uptake) capacities and more complete chemical equilibration. Adsorption capacity is essentially a function of tissue permeability (histological structure) and the available crystalline surface area (crystal size and form), both of which are critical factors in determining the potential for retaining [near] primary geochemical signatures. This is supported by the even higher concentrations of Y, REE, Pb, Th and U within contemporaneous phosphatic brachiopods and ichthyoliths, and their distinct linear correlations between all taxa, with conodont albid crown representing the low concentration end-member and basal tissue or ichthyoliths the high concentration end-members (Figs. 6b–c, e–f, and 7). Further, hyaline tissue shows consistent correlations between Y, REE, Pb, U, and Ba, which are often represented in pore waters, as well as a broad range of other trace metals (see Section 3.1.3) across most localities. Such compositional trends are consistent with a greater propensity for postmortem uptake by hyaline tissues compared to albid crown.

Some ichthyolith tissues (e.g. dermal structures, bone, and tooth dentine) have a highly permeable microstructure comprising an intricate network of vascular canals (Fig. 4b–c) hence often yield geochemical signals derived from secondary overprinting (Elderfield and Pagett, 1986; Toyoda and Tokonami, 1990; Bertram et al., 1992; Koch et al., 1992; Cummins and Elderfield, 1994; Trueman et al., 2003; Martin and Scher, 2004). Phosphatic inarticulate brachiopod valves have also been shown to be unreliable chemical tracers due to their susceptibility to recrystallisation (Wenzel et al., 2000; Pucéat et al., 2004), having an inherently permeable microstructure (punctae in many taxa), high surface to volume ratio, and short diffusion distances. Furthermore, the significant carbonate component within inarticulate brachiopod shell, vertebrate bone, and even tooth dentine increases their susceptibility to dissolution and chemical exchange.

In addition to their contrasting crystalline structures, the relative carbonate contents of conodont tissues may also contribute to observed differences in postmortem uptake. FTIR spectra obtained for representative conodont histologies reveal significant carbonate in basal bodies, lesser amounts in hyaline tissue, and is undetectable in albid crown (Fig. 10), consistent with earlier suggestions of the lower CO_3 content (Pietzner et al., 1968) and lower solubility of albid tissue. Furthermore, the very large crystals (100's μm) comprising cancellate albid crown, as recently discovered by electron diffraction analyses (Trotter et al., submitted for publication), provide both fewer diffusion pathways and minimal surface area for adsorption (exchange) of chemical species. This contrasts with the tiny crystal size and evidence of pore connectivity within lamellar hyaline crown, as indicated by the presence of secondary precipitates (Fig. 2). Similar observations have been made in fossil vertebrate mineralised tissues where diagenetic enrichments are concentrated in bone and tooth dentine, which are considerably more permeable than the structurally denser enamel. The significantly larger and densely packed crystals, as well as the lower carbonate content of enamels (and enameloids), reduce hydraulic conductivity thus retarding element transport and adsorption onto the apatite crystallites during diagenesis (Fig. 4a). Although dense enamels are the preferred tissue for geochemical analysis (Ayliffe et al., 1994; Cerling and Sharp, 1996;

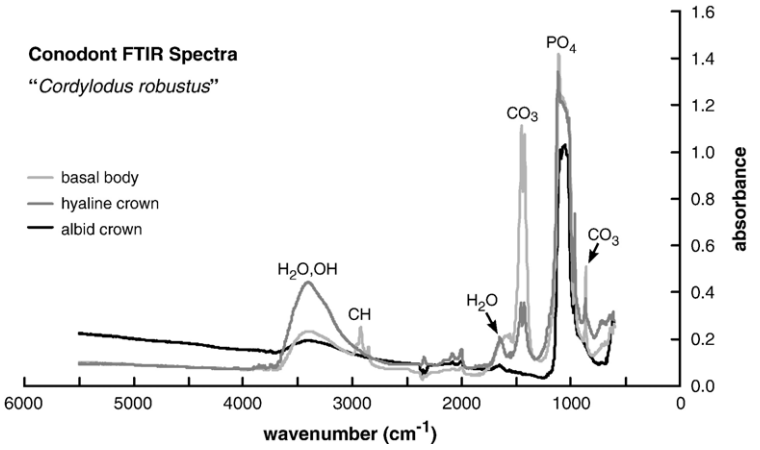

Fig. 10. Representative FTIR spectra for basal body, hyaline, and albid crown conodont tissues of "*Cordylodus robustus*" showing characteristic CO_3, H_2O (+OH), CH, and PO_4 absorption bands. Note that saturation of the main absorbance PO_4 band precluded resolution of its structure, including the 1096 cm^{-1} peak.

Fricke and O'Neil, 1996; Koch et al., 1997; Sharp et al., 2000; Kohn and Cerling, 2002; Eggins et al., 2003; Zazzo et al., 2004) they may also experience chemical alteration.

The presence of organic components in phosphatic tissues is believed to further facilitate the postmortem uptake and isotopic exchange of various elements (Wright et al., 1990; Ayliffe et al., 1994; Blake et al., 1997; Sharp et al., 2000; Trueman and Tuross, 2002; Trueman et al., 2003; Zazzo et al., 2004). Aside from promoting chemical exchange with pore waters during catalysis, the microbial degradation of organics also provides additional migration pathways for pore fluids which promote recrystallisation. In this context, it is interesting to note that organic molecules (irrespective of their origin) have been found in conodont basal body and hyaline tissues yet are seemingly absent in albid crown (Pietzner et al., 1968; Savage et al., 1990; Kemp and Nicoll, 1996; Kemp, 2002).

An alternative interpretation of albid crown trace element chemistry and its large single crystal structure may invoke recrystallisation during diagenesis accompanied by the removal of CO_3 and REE, the latter having been incorporated postmortem. In this scenario, a growing albid crystal may concentrate rejected REE at and ahead of the recrystallisation front, possibly manifesting as an REE enriched zone in the vicinity of the albid–hyaline junction. No such enrichments have been observed using LA-ICPMS at the transition from hyaline to albid regions in blocked and longitudinally sectioned conodonts, but rather a simple stepped decrease in REE concentrations occurs across the boundary. Low CO_3 contents together with high F order, the latter attributed to diagenetic uptake and represented by an enhanced 1096 cm^{-1} absorbance peak of FTIR spectra, have been correlated with increased crystallinity (CI) of fossil bio-apatites (Shemesh, 1990). However, Pucéat et al. (2004) have recently shown CI to be an unreliable indicator of post-depositional recrystallisation and chemical modification. Furthermore, and as mentioned by Pucéat et al. (2004), the CO_3 and F contents of apatite histologies (bone, dentine, enamel) vary naturally and are taxon-specific among living fish (LeGeros et al., 1978; LeGeros and Suga, 1980; Suga et al., 1980), but could also be influenced by local environmental conditions, such as *p*H (LeGeros, 1981). It should therefore be noted that no significant differences in F contents between conodont crown tissues has been observed and that CO_3 contents are comparatively high in basal bodies, present in hyaline tissues, and absent from albid crown which represents the least permeable conodont histology (Fig. 10). Finally, it is difficult to conceive that albid regions would consistently undergo extensive diagenetic recrystallisation while adjacent permeable hyaline tissue escaped with comparatively little change, retaining a fine, well-preserved, microcrystalline structure. This would require the primary albid tissue to be considerably less stable during diagenesis than adjacent hyaline crown. Accordingly, the high REE contents of hyaline tissues are interpreted as significantly modified by secondary uptake from pore waters, whereas strongly ∪-shaped REE profiles of albid crown reflect inhibited postmortem uptake and chemical exchange, and represent compositions most closely approaching primary conodont apatite. The extent to which this pattern applies to other chemical elements depends on their behaviour during diagenesis in particular.

4.2. Sources of postmortem compositions

The origin of REE abundance patterns in fossil marine bio-apatites is the subject of an ongoing debate, with links to sediment pore waters during early and/or later diagenesis (Elderfield and Pagett, 1986; Sholkovitz et al., 1989; German and Elderfield, 1990; Toyoda and Tokonami, 1990; Trueman et al., 2003) or ambient seawater compositions being proposed (Wright et al., 1984, 1987b; Grandjean et al., 1987; Grandjean-Lécuyer et al., 1993; Girard and Albarède, 1996; Reynard et al., 1999; Armstrong et al., 2001; Girard and Lécuyer, 2002; Picard et al., 2002; Lécuyer et al., 2004). Recent modelling has suggested that strongly MREE enriched ('bell-shaped'), shale-normalised abundance patterns were manifested by chemical substitution during late diagenetic recrystallisation (Reynard et al., 1999), and has been applied to screen significantly altered samples (Girard and Lécuyer, 2002; Picard et al., 2002; Lécuyer et al., 2004).

Shale-normalised REE abundance patterns (Fig. 8) of the Paleozoic samples analysed in this study show variable MREE enrichment patterns similar to those previously described in ancient biogenic apatite (e.g. Wright et al., 1984, 1987b). Studies of modern pore water compositions within subsea sediments and interactions at the sediment–water interface have determined a broad and variable range in REE abundance patterns that do not represent the overlying seawater composition (Elderfield and Sholkovitz, 1987; Sholkovitz et al., 1989; Haley et al., 2004). It is notable that conspicuous MREE enriched patterns reminiscent of many fossil bio-apatite REE data including those of this study have only recently been shown to characterise pore waters within an Fe-rich anoxic zone of the sediment column (Haley et al., 2004). In addition, the HREE enriched seawater-like pattern of the Holocene ichthyolith sample (Figs. 4c and 8b) does not reflect ambient seawater composition as the negative Ce anomaly is absent.

The observed ranges in published pore water compositions suggest that it may now be more appropriate to attribute variations in REE abundance patterns (including MREE enriched profiles) of fossil marine bio-apatites to differences in pore water composition, with variations reflecting differences in depth of burial, stage of diagenesis, and depositional environment. REE abundance patterns may potentially but indirectly reflect the dominant processes occurring throughout the water column and subsea sediments, assuming that subsequent overprinting of initial patterns is insignificant which is dependent on sample permeability and its diagenetic history.

5. Conclusions

This study demonstrates that LA-ICPMS is well-suited for in-situ characterisation of conodont geochemistry, yielding continuous compositional depth profiles through individual conodont elements with high-spatial resolution. The systematic differences in Y, REE, Pb, Th, and U concentrations between conodont tissues, ichthyoliths, and phosphatic brachiopods are interpreted to reflect postmortem uptake of these elements as a consequence of the relative permeability and differing crystalline structure of these bio-apatites. Significantly lower concentrations and the ∪-shaped profiles of albid crown contrast with the enriched and typically uniform (equilibrated) profiles of hyaline and basal body conodont tissues, the latter being similar to contemporaneous ichthyolith and brachiopod profiles and concentrations. The strong linear correlation between the REE compositions of these histologies defines albid crown as the low concentration end-member that suffers the least chemical overprinting postmortem. Accordingly, albid crown is inferred to be the least permeable histology and offers the most potential for preserving [near] primary bio-apatite compositions.

The particularly high concentrations of many elements in basal body tissues (and cavities) highlight the necessity to target appropriate taxa to minimize contamination. Sample selection should therefore avoid most panderodontids, especially those with deep basal cavities, but also with respect to the inherent structural weakness of the longitudinal furrow that may serve as a conduit for fluid and dissolved element migration. It is proposed that large albid denticles and cusps should be targeted in preference to hyaline crown if [near] primary bio-apatite compositions are sought, which requires physical separation of these components for bulk and wet chemical techniques. For pore water REE studies, hyaline tissue is more suitable due to its greater capacity for adsorbing high concentrations of REE compared to albid crown, however, the relationship between pore water composition and large-scale seawater signals remains ambiguous.

This study cautions against the indiscriminate use of fossil biogenic apatite as a paleoproxy for ambient seawater chemistry and has identified potential sources of contamination and histologies more susceptible to diagenesis. LA-ICPMS profiles together with recent TEM observations (Trotter et al., submitted for publication) suggest the need to consider tissue ultrastructure and sample permeability in the context of diagenesis, to determine its potential for retaining

primary geochemical signatures. In-situ screening and/or analysis by laser ablation profiling can be used to better constrain the diagenetic history and integrity of the target sample.

Acknowledgements

The authors gratefully acknowledge Christopher Barnes (University of Victoria, BC, Canada), Robert Nicoll (Department of Earth and Marine Sciences, The Australian National University), Cindy Wright (Institute of Ocean Sciences, Sidney, BC, Canada), and Michael Kingsford (James Cook University, Australia) for providing fossil and modern bio-apatites for analysis. Technical assistance from Michael Shelley and Charlotte Allen (Research School of Earth Sciences, ANU) with LA-ICPMS operation is gratefully acknowledged. Andrew Berry (Research School of Earth Sciences, ANU) provided assistance with FTIR samples analysis. Malcolm McCulloch (Research School of Earth Sciences, ANU) is also thanked for informative discussion and editorial comments on the manuscript. Ellen Martin and Jan Kosler are thanked for constructive reviews. Gilbert Klapper kindly provided a copy of Hedy Dechert's English translation of Pietzner et al. (1968). This research was funded by an Australian Postgraduate Award, and support from a student award granted by the Paleontological Society and Mid-American Paleontological Society is also acknowledged. **[RR]**

Appendix A. Supplementary data

Supplementary data associated with this article can be found, in the online version, at doi:10.1016/j.chemgeo.2006.03.004.

References

Armstrong, H.A., Pearson, D.G., Griselin, M., 2001. Thermal effects on rare earth element and strontium isotope chemistry in single conodont elements. Geochimica et Cosmochimica Acta 65 (3), 435–441.

Austin, R.L. 1987. Conodonts: Investigative Techniques and Applications. British Micropaleontological Society, Ellis Horwood Press. 422 pp.

Ayliffe, L.K., Chivas, A.R., Leakey, M.G., 1994. The retention of primary oxygen isotope compositions of fossil elephant skeletal phosphate. Geochimica et Cosmochimica Acta 58 (23), 5291–5298.

Bernat, M., 1975. Les isotopes de l'uranium et du thorium et les terres rares dans l'environment marin. Cahiers - ORSTOM. Série Géologie 7, 65–83.

Bertram, C.J., Elderfield, H., Aldridge, R.J., Conway Morris, S., 1992. $^{87}Sr/^{86}Sr$, $^{143}Nd/^{144}Nd$ and REES in Silurian phosphatic fossils. Earth and Planetary Science Letters 113 (1–2), 239–249.

Blake, R.E., O'Neil, J.R., Garcia, G.A., 1997. Oxygen isotope systematics of biologically mediated reactions of phosphate: I. Microbial degradation of organophosphorus compounds. Geochimica et Cosmochimica Acta 61 (20), 4411–4422.

Bradshaw, L.E., Noel, J.A., Larson, R.J., 1972. Neutron activation analysis of selected conodonts. In: Rhodes, F.H.T. (Ed.), Conodont Paleozoology. Geological Society of America, Special Paper, 141, p. 296. Boulder.

Bruhn, F., Meijer, J., Stephan, A., Korte, C., Veizer, J., 1997. Trace element concentrations in conodonts measured by the Bochum proton microprobe. Nuclear Instruments and Methods in Physics Research Section B: Beam Interactions with Materials and Atoms 130 (1–4), 636–640.

Cerling, T.E., Sharp, Z.D., 1996. Stable carbon and oxygen isotope analysis of fossil tooth enamel using laser ablation. Palaeogeography, Palaeoclimatology, Palaeoecology 126 (1–2), 173–186.

Cummins, D.I., Elderfield, H., 1994. The strontium isotopic composition of Brigantian (late Dinantian) seawater. Chemical Geology 118, 255–270.

Diener, A., Ebneth, S., Veizer, J., Buhl, D., 1996. Strontium isotope stratigraphy of the Middle Devonian: brachiopods and conodonts. Geochimica et Cosmochimica Acta 60 (4), 639–652.

Donoghue, P.C.J., 1998. Growth and patterning in the conodont skeleton. Philosophical Transactions of the Royal Society of London-Series B: Biological Sciences 353 (1368), 633–666.

Ebneth, S., Diener, A., Buhl, D., Veizer, J., 1997. Strontium isotope systematics of conodonts: Middle Devonian, Eifel Mountains, Germany. Palaeogeography, Palaeoclimatology, Palaeoecology 132 (1–4), 79–96.

Ebneth, S., Shields, G.A., Veizer, J., Miller, J.F., Shergold, J.H., 2001. High-resolution strontium isotope stratigraphy across the Cambrian–Ordovician transition. Geochimica et Cosmochimica Acta 65 (14), 2273–2292.

Eggins, S.M., Woodhead, J.D., Kinsley, L.P.J., Mortimer, G.E., Sylvester, P., McCulloch, M.T., Hergt, J.M., Handler, M.R., 1997. A simple method for the price determination of ≥40 trace elements in geological samples by ICPMS using enriched isotope internal standardisation. Chemical Geology 134, 311–326.

Eggins, S.M., Rudnick, R.L., McDonough, W.F.M., 1998a. The composition of peridotites and their minerals, a laser-ablation ICPMS study. Earth and Planetary Science Letters 154, 53–71.

Eggins, S.M., Kinsley L.K., Shelley J.M.G., 1998b. Deposition and element fractionation processes occurring during atmospheric pressure laser sampling for analysis by ICPMS. Applied Surface Science 127–129, 278–286.

Eggins, S., Grün, R., Pike, A., Shelley, A., Taylor, L., 2003. ^{238}U, ^{232}Th profiling and U-series isotope analysis of fossil teeth by laser ablation-ICPMS. Quaternary Science Reviews 22, 1373–1382.

Eggins, S.M., Sadekov, A., DeDeckker, P., 2004. Modulation and daily banding of Mg/Ca in *Orbulina universa* tests by symbiont photosynthesis and respiration: a complication for seawater thermometry. Earth and Planetary Science Letters 225, 411–419.

Elderfield, H., Pagett, R., 1986. Rare earth elements in ichthyoliths: variations with redox conditions and depositional environments. Science of the Total Environment 49, 175–197.

Elderfield, H., Sholkovitz, E.R., 1987. Rare earth elements in the pore waters of reducing nearshore sediments. Earth and Planetary Science Letters 82, 280–288.

Epstein, A.G., Epstein, J.B., Harris, L.D., 1977. Conodont color alteration—an index to organic metamorphism. U.S. Geological Survey Professional Paper 995, 1–27.

Felitsyn, S., Sturesson, U., Popov, L., Holmer, L., 1998. Nd isotope composition and rare earth element distribution in early Paleozoic biogenic apatite from Baltoscandia: a signature of Iapetus ocean water. Geology 26 (12), 1083–1086.

Fricke, H.C., O'Neil, J.R., 1996. Inter- and intra-tooth variation in the oxygen isotope composition of mammalian tooth enamel phosphate: implications for palaeoclimatological and palaeobiological research. Palaeogeography, Palaeoclimatology, Palaeoecology 126 (1–2), 91–99.

Geitgey, J.E., Carr, T.R., 1987. Temperature as a factor affecting conodont diversity and distribution. In: Austin, R.L. (Ed.), Conodonts: Investigative Techniques and Applications. Ellis Horwood Ltd., Chichester, pp. 241–255.

German, C.R., Elderfield, H., 1990. Application of the Ce anomaly as a paleoredox indicator: the ground rules. Paleoceanography 5 (5), 823–833.

Girard, C., Albarède, F., 1996. Trace elements in conodont phosphates from the Frasnian/Famennian boundary. Palaeogeography, Palaeoclimatology, Palaeoecology 126 (1–2), 195–209.

Girard, C., Lécuyer, C., 2002. Variations in Ce anomalies of conodonts through the Frasnian/Famennian boundary of Poland (Kowala—Holy Cross Mountains): implications for the redox state of seawater and biodiversity. Palaeogeography, Palaeoclimatology, Palaeoecology 181 (1–3), 299–311.

Grandjean, P., Cappetta, H., Michard, A., Albarède, F., 1987. The assessment of REE patterns and $^{143}Nd/^{144}Nd$ ratios in fish remains. Earth and Planetary Science Letters 84 (2–3), 181–196.

Grandjean-Lécuyer, P., Feist, R., Albarède, F., 1993. Rare earth elements in old biogenic apatites. Geochimica et Cosmochimica Acta 57, 2507–2514.

Haley, B.A., Klinkhammer, G.P., McManus, J., 2004. Rare earth elements in pore waters of marine sediments. Geochimica et Cosmochimica Acta 68 (6), 1265–1279.

Holmden, C., Creaser, R.A., Muehlenbachs, K., Bergström, S.M., Leslie, S.A., 1996. Isotopic and elemental systematics of Sr and Nd in 454 Ma biogenic apatites: implications for paleoseawater studies. Earth and Planetary Science Letters 142, 425–437.

Holmden, C., Creaser, R.A., Muehlenbachs, K., Leslie, S.A., Bergström, S.M., 1998. Isotopic evidence for geochemical decoupling between ancient epeiric seas and bordering oceans: implications for secular curves. Geology 26 (6), 567–570.

Jahnke, R.A., 1984. The synthesis and solubility of carbonate fluorapatite. American Journal of Science 284, 58–78.

Joachimski, M.M., Buggisch, W., 2002. Conodont apatite ^{18}O signatures indicate climatic cooling as a trigger of the Late Devonian mass extinction. Geology 30 (8), 711–714.

Joachimski, M.M., van Geldern, R., Breisig, S., Buggisch, W., Day, J., 2004. Oxygen isotope evolution of biogenic calcite and apatite during the Middle and Late Devonian. International Journal of Earth Sciences 93 (4), 542–553.

Kemp, A.J., 2002. Hyaline tissue of thermally unaltered conodont elements and the enamel of vertebrates. Alcheringa 23–36.

Kemp, A.J., Nicoll, R.S., 1996. A histochemical analysis of biological residues in conodont elements. Modern Geology 20, 287–302.

Keto, L.S., Jacobsen, S.B., 1987. Nd and Sr isotopic variations of early Paleozoic oceans. Earth and Planetary Science Letters 84 (1), 27–41.

Koch, P.L., Halliday, A.N., Walter, L.M., Stearley, R.F., Huston, T.J., Smith, G.R., 1992. Sr isotopic composition of hydroxyapatite from recent and fossil salmon: the record of lifetime migration and diagenesis. Earth and Planetary Science Letters 108, 277–287.

Koch, P.L., Tuross, N., Fogel, M.L., 1997. The effects of sample treatment and diagenesis on the isotopic integrity of carbonate in biogenic hydroxyapatite. Journal of Archaeological Science 24 (5), 417–429.

Kohn, M.J., Cerling, T.E., 2002. Stable isotope compositions of biological apatite. In: Kohn, M.J., Rakovan, J., Hughes, J.M. (Eds.), Phosphates—Geochemical, Geobiological and Materials Importance. Reviews in Mineralogical Geochemistry, vol. 48. Mineralogical Society of America, Washington, DC, pp. 455–480.

Kohn, M.J., Schoeninger, M.J., Barker, W.W., 1999. Altered states: effects of diagenesis on fossil tooth chemistry. Geochimica et Cosmochimica Acta 63 (18), 2737–2747.

Kürschner, W., Becker, R.T., Buhl, D., Veizer, J., 1992. Strontium isotopes in conodonts: Devonian–Carboniferous transition, the northern Rhenish Slate Mountains, Germany. Annales de la Societe Geologique de Belgique 115 (2), 595–621.

Lécuyer, C., Reynard, B., Grandjean, P., 2004. Rare earth element evolution of Phanerozoic seawater recorded in biogenic apatites. Chemical Geology 204 (1–2), 63–102.

LeGeros, R.Z., 1981. Apatites in biological systems. Progress in Crystal Growth and Characterization 4 (1–2), 1–45.

LeGeros, R.Z., Suga, S., 1980. Crystallographic nature of fluoride in enameloids of fish. Calcified Tissue International 32, 169–174.

LeGeros, R.Z., Go, P., Suga, S., 1978. Fluoride in fish enameloids. Journal of Dental Research 57A, 280.

Longerich, H.P., Jackson, S.E., Günther, D., 1996. Laser ablation inductively couples plasma mass spectrometry transient signal data acquisition and analyte concentration calculation. Journal of Analytical Atomic Spectrometry 11, 899–904.

Luz, B., Kolodny, Y., Kovach, J., 1984. Oxygen isotope variations in phosphate of biogenic apatites: III. Conodonts. Earth and Planetary Science Letters 69 (2), 255–262.

Martin, E.E., Macdougall, J.D., 1995. Sr and Nd isotopes at the Permian/Triassic boundary: a record of climate change. Chemical Geology 125, 73–99.

Martin, E.E., Scher, H.D., 2004. Preservation of seawater Sr and Nd isotopes in fossil fish teeth: bad news and good news. Earth and Planetary Science Letters 220 (1–2), 25–39.

McConnell, D., 1973. Apatite: Its Crystal Chemistry, Mineralogy, Utilization, and Geologic and Biologic Occurrences. Springer-Verlag, Wien, New York.

McLennan, S.M., 1989. Rare earth elements in sedimentary rocks: influence of prevenance and sedimentary processes. In: Lipin, B. R., McKay, G.A. (Eds.), Reviews in Mineralogy. Mineralogical Society of America, Washington, pp. 170–200.

Millard, A.R., Hedges, R.E.M., 1996. A diffusion–adsorption model of uranium uptake by archaeological bone. Geochimica et Cosmochimica Acta 60 (12), 2139–2152.

Pearce, N.J.G., Perkins, W.T., Westgate, J.A., Gorton, M.J., Jackson, S.E., Neale, C.R., Chenery, S.J., 1997. A compilation of new and published major and trace element data for NIST SRM 610 and NIST SRM 612 glass reference materials. Geostandards Newsletter Journal of Geostandards and Geoanalysis 21, 115–144.

Picard, S., Lécuyer, C., Barrat, J., Garcia, J., Dromart, G., Sheppard, S. M.F., 2002. Rare earth element contents of Jurassic fish and reptile teeth and their potential relation to seawater composition (Anglo-Paris Basin, France and England). Chemical Geology 186 (1–2), 1–116.

Pietzner, H., Vahl, J., Werner, H., Ziegler, W., 1968. Zur chemischen zusammensetzung und mikromorphologie der conodonten. Palaeontographica Abteilung A 128 (4–6), 115–152.

Pike, A.W.G., Hedges, R.E.M., 2001. Sample geometry and U uptake in archaeological teeth: implications for U-series and ESR dating. Quaternary Science Reviews 20 (5–9), 1021–1025.

Pucéat, E., Reynard, B., Lécuyer, C., 2004. Can crystallinity be used to determine the degree of chemical alteration of biogenic apatites? Chemical Geology 205 (1–2), 83–97.

Reynard, B., Lecuyer, C., Grandjean, P., 1999. Crystal-chemical controls on rare-earth element concentrations in fossil biogenic apatites and implications for paleoenvironmental reconstructions. Chemical Geology 155 (3–4), 233–241.

Ruppel, S.C., James, E.W., Barrick, J.E., Nowlan, G., Uyeno, T.T., 1996. High-resolution $^{87}Sr/^{86}Sr$ chemostratigraphy of the Silurian: implications for event correlation and strontium flux. Geology 24 (9), 831–834.

Savage, N.M., Lindorfer, A., McMillan, D.A., 1990. Amino acids from Ordovician conodonts. CFS. Courier Forschungsinstitut Senckenberg 118, 267–275.

Sharp, Z.D., Atudorei, V., Furrer, H., 2000. The effect of diagenesis on oxygen isotope ratios of biogenic phosphates. American Journal of Science 300 (March), 222–237.

Shaw, H.F., Wasserburg, G.J., 1985. Sm–Nd in marine carbonates and phosphates: implications for Nd isotopes in seawater and crustal ages. Geochimica et Cosmochimica Acta 49, 503–518.

Shemesh, A., 1990. Crystallinity and diagenesis of sedimentary apatites. Geochimica et Cosmochimica Acta 54, 2433–2438.

Sholkovitz, E.R., Piepgras, D.J., Jacobsen, S.B., 1989. The pore water chemistry of rare earth elements in Buzzards Bay sediments. Geochimica et Cosmochimica Acta 53 (11), 2847–2856.

Suga, P., Wada, K., Ogawa, M., 1980. Fluoride concentrations in the enameloids of fish. In: Omori, M., Watabe, N. (Eds.), Biomineralisation Mechanisms in Animals and Plants. Tokai Univ. Press, Tokyo, pp. 229–240.

Toyoda, K., Tokonami, M., 1990. Diffusion of rare-earth elements in fish teeth from deep-sea sediments 345 (6276), 607–609.

Trotter, J.A., Korsch, M.J., Nicoll, R.S., Whitford, D.J., 1999. Sr isotopic variation in single conodont elements: implications for defining the Sr seawater curve. In: Sepagli, E. (Ed.), Seventh European Conodont Symposium. Studies on Conodonts. Bolletino Della Societa Paleontologica Italiana, Bologna-Modena, pp. 507–514.

Trotter, J.A., Fitz Gerald, J.D., Kokkonen, H., Barnes, C.R. submitted for publication. Ultrastructure, permeability, and integrity of conodont apatite determined by Transmission Electron Microscopy. Lethaia.

Trueman, C.N., Tuross, N., 2002. Trace elements of recent and fossil bone apatite. In: Kohn, M.J., Rakovan, J., Hughes, J.M. (Eds.), Phosphates—Geochemical, Geobiological and Materials Importance. Reviews in Mineralogical Geochemistry, vol. 48. Mineralogical Society of America, Washington, DC, pp. 489–521.

Trueman, C.N., Benton, M.J., Palmer, M.R., 2003. Geochemical taphonomy of shallow marine vertebrate assemblages. Palaeogeography, Palaeoclimatology, Palaeoecology 197 (3–4), 151–169.

Vennemann, T.W., Hegner, E., Cliff, G., Benz, G.W., 2001. Isotopic composition of recent shark teeth as a proxy for environmental conditions. Geochimica et Cosmochimica Acta 65 (10), 1583–1599.

Wenzel, B., Lécuyer, C., Joachimski, M.M., 2000. Comparing oxygen isotope records of Silurian calcite and phosphate—$\delta^{18}O$ compositions of brachiopods and conodonts. Geochimica et Cosmochimica Acta 64 (11), 1859–1872.

Wright, J., Seymour, R.S., Shaw, H.F., 1984. REE and Nd isotopes in conodont apatite: variations with geological age and depositional environment. In: Clark, D.L. (Ed.), Conodont Biofacies and Provincialism. Geological Society of America Special Paper, pp. 325–340.

Wright, J., Miller, J.F., Holser, W.T., 1987a. Conodont chemostratigraphy across the Cambrian–Ordovician boundary: western USA and southeast China. In: Austin, R.L. (Ed.), Conodonts: Investigative Techniques and Applications. Ellis Howard, Chichester, pp. 259–286.

Wright, J., Schrader, H., Holser, W.T., 1987b. Paleoredox variations in ancient oceans recorded by rare earth elements in fossil apatite. Geochimica et Cosmochimica Acta 51, 631–644.

Wright, J., Conca, J.L., Repetski, J.E., Clark, J., 1990. Microgeochemistry of some lower Ordovician cordylodans from Jilin, China. CFS. Courier Forschungsinstitut Senckenberg 118, 307–331.

Wright, C.A., Barnes, C.R., Jacobsen, S.B., 2002. The neodymium isotopic composition of Ordovician conodonts as a seawater proxy: testing paleogeography. Geochemistry, Geophysics, Geosystems 3 (2), doi:10.1029/2001GC000195.

Zazzo, A., Lecuyer, C., Mariotti, A., 2004. Experimentally-controlled carbon and oxygen isotope exchange between bioapatites and water under inorganic and microbially-mediated conditions. Geochimica et Cosmochimica Acta 68 (1), 1–12.